

Anticancer Effects of *Gleditsia sinensis* Extract in Rats Transplanted With Hepatocellular Carcinoma Cells

Yue Cai,*†‡ Chizhi Zhang,*†‡ Lei Zhan,*† Liangbin Cheng,*† Dingbo Lu,*† Xiaodong Wang,*† Hanlin Xu,§ Shuxue Wang,¶ Deng Wu,*† and Lianguo Ruan#

*Clinical Medical College of Hubei University of Chinese Medicine, Wuhan, P.R. China

†Department of Hepatology, Hubei Provincial Hospital of Traditional Chinese Medicine, Wuhan, P.R. China

‡Hubei Province Academy of Traditional Chinese Medicine, Wuhan, P.R. China

§College of Pharmacy of Hubei University of Chinese Medicine, Wuhan, P.R. China

¶Wuhan Hospital of Traditional Chinese Medicine Department of Pediatrics, Wuhan, P.R. China

#Infectious Disease of Wuhan Medical Treatment Center, Wuhan, P.R. China

The thorns of *Gleditsia sinensis* have been historically used in Chinese medicine and are considered one of the fundamental therapeutic herbs. Its anticancer effects are currently being explored. Hepatocellular carcinoma (HCC) is the most common type of primary liver cancer and still requires the development of new drugs with higher efficiency. By using a rat HCC model implanted with cancerous Walker-256 cells, the therapeutic effects of *G. sinensis* extract (GSE) were assessed, as well as its regulatory effects on miRNAs. GSE significantly restored liver morphology and dramatically induced cell apoptosis in HCC rats. In addition, miR-21/181b/183 was upregulated in the HCC liver, and the elevation of these miRNAs could be alleviated by both GSE and sorafenib. PTEN/TIMP3/PDCD4 downregulation was consistent with the targets of miR-21/181b/183 in the HCC liver, and the alteration of these target genes was restored by both GSE and sorafenib. TIMP3 effects on MMP-2/9 expression were also determined. Our present findings indicate the potential of GSE in HCC treatment, and expand the understanding of miRNA-related mechanisms in the anticancer effects of GSE.

Key words: *Gleditsia sinensis* extract (GSE); Anticancer; Hepatocellular carcinoma (HCC); Gene expression

INTRODUCTION

Gleditsia species are used as traditional medicines in many world cultures for a number of diseases. These plants are found in Central and Southeast Asia, as well as in North and South America. The thorns of *Gleditsia sinensis* (FGS), also known as Chinese honey locust, soap bean, or soap pod, are historically used as a traditional Chinese medicine for their anti-inflammatory, antiseptic, and anti-tumor properties¹. More than 60 compounds, including triterpenes, sterols, flavonoids, alkaloids, and phenolics and their derivatives have been isolated from the crude extracts, in addition to purified molecules from *Gleditsia* species, which exhibit diverse cytoprotective activities²⁻⁴.

Recent studies have reported the anticancer effects of *G. sinensis*. For instance, Kim et al.⁵ reported that the fruit hull of FGS enhances the effectiveness of the chemotherapeutic drug cisplatin for lung cancer in both

in vitro test for apoptosis and cell cycle of Lewis lung carcinoma (LLC) cells, and in vivo experiments for the reduction of LLC-derived lung tumor growth. Ryu et al.⁶ reported that the water extract of *G. sinensis* thorns significantly suppresses PC3 prostate cancer cell migration in vitro by attenuating collagen against adhesion, while its oral administration inhibits PC3 cell xenografted tumor growth. It was also observed that the ethanolic extract of *G. sinensis* thorns and its active constituent cytochalasin H have antiangiogenic effects in vitro and in vivo by suppressing endothelial cell functions⁷. The saponin fraction of the fruit extract from *Gleditsia caspica*, a relative of *G. sinensis* with similar saponins, was shown to inhibit chromosomal aberrations induced by cyclophosphamide (CP), with cytotoxic effects in human breast cancer MCF-7 cells⁸.

Hepatocellular carcinoma (HCC) is the most common type of primary liver cancer and frequently occurs in

Address correspondence to Chizhi Zhang, Clinical Medical College of Hubei University of Chinese Medicine, No. 1 Huangjiahu East Road, Hongshan District, Wuhan 430065, P.R. China. E-mail: zhangchizhi@126.com

patients with underlying chronic liver disease and cirrhosis. The thorns of *G. sinensis* are also effective in liver cancer cell lines⁹. However, the molecular mechanisms underlying these therapeutic effects remain unclear, preventing its further development as a first-line anticancer drug.

The pathogenesis of HCC involves microRNAs (miRNAs). Currently, there are nearly 2,000 publications in the PubMed database reporting how miRNAs contribute to HCC development; detailed reviews suggest an miRNA-based therapy for HCC¹⁰. The miRNA profile exhibits substantial change during tumorigenesis, and certain critical miRNAs play indispensable roles in controlling tumor cell growth and viability, and could also regulate the tumor microenvironment by affecting stroma–tumor communication¹¹.

Given the therapeutic potential of *G. sinensis* in liver tumor cell lines, and the involvement of miRNAs in the pathogenesis of HCC, it would be interesting to explore how, if at all, miRNAs mediate the anticancer effects of *G. sinensis* in HCC. In the current study, we report that *G. sinensis* extract protects the liver from oncogenic injury in a rat tumor transplantation model. We identified multiple miRNAs that were altered in this model, and certain important targets of these differentially regulated miRNAs were found to be linked to the development of HCC in our model.

MATERIALS AND METHODS

Animals

A total of five clean-grade male weaned Wistar rats, with body weights of 70–100 g, were purchased from Hubei Experimental Animal Research Center for cancer cell proliferation and passage. In addition, 65 clean-grade male SD rats from the same center, with body weights of 180–229 g, were used for the establishment of the HCC model. This research was reviewed by the ethics committee of Hubei University of Chinese Medicine. It was found that the research was in line with the “regulations on the management of experimental animals,” and could provide them with adequate and healthy diet and drinking water, reduce their pain and suffering, and the application of experimental animals for scientific research conforms to the internationally accepted animal welfare and ethical norms.

Cell Culture

The Walker-256 cancer cell line, purchased from Shanghai Bioleaf Biotech Co., Ltd. (P.R. China), was cultured in Dulbecco's modified Eagle's medium (DMEM; Gibco, Gaithersburg, MD, USA), supplemented with 10% NCS and 50 µg/ml of kanamycin (Gibco).

Gleditsia sinensis Extraction

G. sinensis herb was purchased from Hubei Medicinal Material Company (P.R. China). Professor Hezhen Wu

from the Department of Traditional Chinese Medicine Identification, Hubei University of Traditional Chinese Medicine, identified the herb to be the dried fruit of *G. sinensis* Lam, certified genuine by the 2010 edition of the Chinese Pharmacopoeia. Extracting the *n*-butanol fraction from *G. sinensis* was performed by the School of Pharmacy, Hubei University of Traditional Chinese Medicine. First, 30 kg of raw *G. sinensis* was dried, ground, and filtered through a 40N mesh, followed by three ethanol extractions. Then the ethanol was recovered under low pressure, and a total of 3,984 g of ethanol-free extract (crude drug) was obtained and steamed on a rotating evaporator until it became viscous. This process yielded about 800 ml of *G. sinensis* concentrate, and fractional extraction using *n*-butanol was further performed to remove lipid components and other impurities. The concentrate was extracted eight times, with 1,000 ml of *n*-butanol for 4 h each, until the solution became colorless. The extract was collected and concentrated, and the *n*-butanol fraction from *G. sinensis* was finally prepared.

Establishment of the Rat HCC Model

Walker-256 cells $>1 \times 10^6$ /ml were resuspended and transferred into a 15-ml centrifuge tube, which was gently shaken and supplemented with 8 ml of PBS. The suspension was centrifuged for 10 min at 1,000 rpm, and the cell pellet was rinsed twice with PBS and resuspended in 4 ml of PBS. With a 5-ml syringe, the cell suspension was injected into the peritoneal cavity of five Wistar rats at a volume of 1 ml; after 20 days, the rats showed abdominal distention and formation of cancerous ascites.

Then 15 ml of cancerous ascites was aspirated from the Wistar rats. The sampled ascites were centrifuged for 2 min at 2,000 rpm, and the low viscosity concentrated ascites fluid was collected, rinsed three times with PBS, and diluted to a cell density of 2×10^7 /ml for later use.

Sixty-five SD rats (about 200 g) were separated into six groups ($N=10$) according to body weight, including the control ($N=12$), model ($N=13$), high-dose *G. sinensis* extract (HD extract, $N=10$), medium-dose *G. sinensis* extract (MD extract, $N=10$), low-dose *G. sinensis* extract (LD extract, $N=10$), and sorafenib ($N=10$) groups. Rats were fasted for 12 h before the experiments. Except for the control group, the other five groups were anesthetized with intraperitoneal injection of chloral hydrate (Wuhan Biofavor Biotech Service Co., Ltd., P.R. China) at 40 µg/100 g body weight and immobilized on the operation plate in the supine position; abdominal disinfection was carried out with 0.5% iodine. An incision along the linea alba was made, and the tissues were separated layer by layer to expose the rat's abdominal cavity; the liver was shown bulging above the upper abdomen. The outermost hepatic lobe was selected, and a syringe containing 1 ml of cancerous ascites was obliquely inserted into the lobe at

a depth of 0.5 cm, and about 0.15 ml of cancerous ascites was injected into the liver tissue¹². After rapidly removing the syringe, a sterilized cotton swab was pressed on the puncture until bleeding stopped. The liver was returned to the abdominal cavity, and the wound was sutured and sterilized by applying erythromycin ointment.

To verify whether the model has been established successfully, on the seventh day after modeling, three rats were randomly selected from the 53 modeled rats, and two were selected from the 12 normal rats. The liver tissues of these five rats were sampled for pathological examination.

Grouping for Experiments

The remaining 50 SD rats (around 200 g) were divided into five groups ($N=10$) as described above. Based on the clinical dose for an adult human (crude *G. sinensis* extract at 1.5 g/70 kg/day), the gavage dose in this study utilized the equivalent dose calculated by the ratio of the body surface area between an adult human and a rat; the conversion coefficients are listed in the formulas below:

Seventy kilograms was taken as the average weight of an adult human and 200 g as the average weight of rat

$$\text{Adult human dose of } G. \text{ sinensis extract} = 3 \text{ g}/70 \text{ kg} = 42.857 \text{ mg/kg}$$

$$\text{Experimental dose in rat (mg/kg)} = \text{human dose (mg/kg)} \times (\text{human conversion coefficient}/\text{rat conversion coefficient}) = 42.857 \text{ (mg/kg)} \times (36/6) = 257.14 \text{ (mg/kg)}$$

Setting the ratio between low, medium, and high dose at 1:2:4, the amounts of extract injected to the rats were, respectively, calculated as 128.57 mg/kg/day for the LD extract group, 257.14 mg/kg/day for the MD extract group, and 514.28 mg/kg/day for the HD extract group. Sorafenib (Bayer Pharmaceutical, Elberfeld, Germany) was given at a dose of 68.57 mg/kg/day, which was equivalent to 0.8 g/day in a human adult. The control group was injected with 0.9% physiologic saline at 10 ml/kg/day, and the same treatment was applied in the model group. The volume of gavage was the same in all groups. The treatment started at 1 week after modeling, lasted for 28 days, and was terminated on the 35th day.

Tissue Sampling

Rats were sacrificed by cervical dislocation before tissue sampling. Under aseptic conditions, the rat's abdomen was cut open after skin disinfection. In the control group, the structurally intact part of the liver was sampled. In model groups, intrahepatic cancer tissues were selected; if rats had liver cancer nodules, the tissue with the largest nodule was chosen. Tissues sampled from different groups were dried with filter paper, cut into 1 cm × 1 cm × 0.2 cm blocks, consecutively sectioned,

fixed for 3 h in formalin and ethanol, automatically dehydrated, and used to prepare sections for hematoxylin and eosin (H&E) staining and TUNEL assay.

H&E Staining

Tissue sections were submitted to dehydration, permeabilization, paraffin embedding, slicing, microwaving, deparaffinization, H&E staining, and finally mounted with neutral gum.

TUNEL Staining for Apoptosis Detection

TUNEL staining was performed with an apoptosis detection kit (Roche Applied Science, Indianapolis, IN, USA). Tissue sections were dewaxed and digested using protease K. Samples in test groups were added with 50 μ l of TUNEL reaction mixture and incubated at 37°C for 60 min in the dark and further dried. Then the sections were incubated with 50 μ l of converter-POD for 30 min at 37°C, washed with PBS, and developed at room temperature with the DAB color solution (Wuhan Boster Biological Engineering Co., Ltd., P.R. China). Color development was terminated by rinsing with water. Harris hematoxylin restaining was performed, followed by dehydration and permeabilization, air drying, and mounting with neutral gum. Dried sections were observed, and images were acquired under a Nikon E100 biological microscope (Nikon, Tokyo, Japan). For TUNEL staining, six sections with four high-power fields each per group were observed for the assessment of cell apoptosis. Under a microscope, apoptotic cells were colored brown, and quantitative analysis of the cell apoptotic index in HCC was performed using an image analysis software, Image Pro Plus 6.0 (Media Cybernetics, Rockville, MD, USA).

Real-Time (RT)-PCR

According to the manufacturer's instructions, tissue samples (30 mg) were homogenized thoroughly in liquid nitrogen and added with 1 ml of TRIzol reagent (Invitrogen, Thermo Fisher Scientific, Waltham, MA, USA). RNA quality was analyzed by agarose gel electrophoresis. cDNA synthesis was performed using first-strand cDNA synthesis kit (Fermentas UAB, Waltham, MA, USA), and specific mRNA quantification was enabled by real-time (RT)-PCR using SYBR green/fluorescein qPCR master mix (2 \times ; Fermentas UAB) on a 7900HT real-time PCR system (ABI, Thermo Fisher Scientific, Waltham, MA, USA). The reaction conditions were one cycle of 50°C for 2 min, and 95°C for 10 min, followed by 40 cycles of 95°C for 30 s and 60°C for 30 s. Primers were synthesized by Invitrogen China (Shanghai), and their sequences are listed in Table 1. The Ct value referred to the number of cycles needed for the fluorescence signal in each reaction tube to reach a defined threshold; $2^{-\Delta\Delta Ct}$ was calculated to represent the relative mRNA expression of target genes.

Table 1. Sequences of Primers

Name	Sequences	Product Length
GAPDH		252 bp
Forward	5'-ACAGCAACAGGGTGGTGGAC-3'	
Reverse	5'-TTTGAGGGTGCAGCGAACTT-3'	
PDCD4		209 bp
Forward	5'-AGGTTGCTAGATAGGCGGTC-3'	
Reverse	5'-GTCTTCTCAAACGCCGTCTC-3'	
TIMP3		203 bp
Forward	5'-GCTGTGCAACTTTGTGGAGA-3'	
Reverse	5'-AGGCGTAGTGTGGACTGA-3'	
MMP2		200 bp
Forward	5'-GTCGCCCATCATCAAGTTCC-3'	
Reverse	5'-GCATGGTCTCGATGGTGTTC-3'	
MMP9		168 bp
Forward	5'-AAAGGTCGCTCGGATGGTTA-3'	
Reverse	5'-GGTAGAGTACTGCTTGCCCA-3'	
PTEN		197 bp
Forward	5'-GGAAAGGACGGACTGGTGTA-3'	
Reverse	5'-TGCCACTGGTCTGTAATCCA-3'	

Western Blotting

Liver tissues were homogenized in RIPA buffer (Beyotime Institute of Biotechnology, Haimen, P.R. China), incubated on ice for 10 min, and centrifuged for 10 min at 12,000 rpm at 4°C. The supernatant was collected for further handling. Protein concentration was quantitated using Bradford (Beyotime Institute of Biotechnology). For the Western blot assay, equal amounts of protein (50 µg) were separated by 8% SDS-PAGE and electrophoretically transferred to polyvinylidene fluoride (PVDF) membranes (Millipore, Billerica, MA, USA). Nonspecific binding sites were blocked with 5% milk powder diluted in TBS containing 0.05% Tween 20 (TBST) for 2 h. Proteins were detected by Western blot using primary antibodies against β-actin (BM0627; Wuhan Boster Biological Technology, Ltd.), TIMP-3 (1:300; SC-6836; Santa Cruz Biotechnology, Santa Cruz, CA, USA), PDCD4 (1:300; SC-27123; Santa Cruz Biotechnology), MMP-9 (1:300; SC-10737; Santa Cruz Biotechnology), PTEN (1:300; SC-6818; Santa Cruz Biotechnology), MMP-2 (1:600; BS1236; Bioworld Technology, Inc. St. Louis Park, MN, USA) at 4°C overnight. Blots were then incubated with horseradish peroxidase-conjugated secondary antibodies (1:50,000; Wuhan Boster Biological Technology, Ltd.) for 2 h. Proteins were detected with the enhanced chemiluminescence reagent (Thermo Fisher Scientific, Rockford, IL, USA). Band intensity was quantified using the Bandscan 5.0 software (Glyko, Novato, CA, USA).

Statistical Analysis

Data were statistically analyzed with SPSS 22.0 (SPSS, Chicago, IL, USA). All measurement data are mean ± SD. One-way ANOVA was applied for comparisons

among the six groups, with LSD analysis for intergroup comparison when data met the standards of normal distribution and homogeneity of variance. When variance was not uniform, adjusted variance analysis was applied (Dunnett's T3 method was used for intergroup comparison). For data with nonnormal distribution, a nonparametric test was performed. Statistical significance was defined by a value of $p < 0.05$.

RESULTS

Effects of *Gleditsia sinensis* Extract on Liver Histopathology in HCC-Bearing Rats

To confirm that the HCC model was successfully established in the rats by implanting cancerous ascites of Walker-256 cells, histopathology of liver tissues from the rats was performed. In contrast to the control group, the structure of hepatic lobules in HCC model rats was damaged, with a large portion replaced with tumor tissues, while the adjacent hepatic lobules were compressed and solidified, with hepatic sinusoid dilation and fibrous hyperplasia in the surrounding areas. The portal area was significantly enlarged, filled with lots of fibroblasts and fiber tissues. Tumor cells were round shaped and active in proliferation, displaying overt atypia, hyperchromatism, and a larger karyoplasmic ratio. Nuclear condensation and fragmentation could be observed in some cells. Tumor cells were distributed in masses, and some showed coagulative necrosis, which was stained as dark red. Representative sections are shown at 100× (Fig. 1A) and 200× (Fig. 1B) magnification.

Under the same conditions, administration of *G. sinensis* extracts or sorafenib could restore the histopathology defects in the liver of HCC model rats, including

disordered arrangement of tumor cells, enlarged cytoplasm and nucleus, and connective tissue hyperplasia. The effects of *G. sinensis* extracts were dose dependent, as only the high-dose treatment caused a significant restoration, as potent as the sorafenib positive control, while middle- and low-dose treatments exhibited only mild effects. Representative sections are shown at 100× (Fig. 1A) and 200× (Fig. 1B) magnification.

Effects of *Gleditsia sinensis* Extracts on Cellular Apoptosis in Rat HCC

To determine if *G. sinensis* extracts suppressed HCC progression in rats by inducing apoptosis, we detected apoptotic cells in liver sections via TUNEL staining. In the control group, there was limited apoptosis detected in liver samples (Fig. 2A). The implantation of cancerous ascites of Walker-256 cells caused HCC-like pathology in the rat liver, where apoptosis was hardly observed, indicating the high viability of cancerous cells in the model liver (Fig. 2A). In contrast, treatment with *G. sinensis*

extracts significantly induced apoptosis in HCC-bearing liver tissues, in a dose-dependent manner. Indeed, all *G. sinensis* extract groups (low, medium, and high) showed significant differences compared with the model group ($p < 0.01$). The high-dose *G. sinensis* extract group was comparable to sorafenib (positive control) administration, causing severe apoptosis in HCC-bearing livers (Fig. 2A and B), with markedly higher apoptotic levels compared with the model group.

Effects of *Gleditsia sinensis* Extracts on miRNAs in HCC-Bearing Rats

As miRNAs were reported to be potential mediators of HCC pathogenesis and could be modulated by anti-cancer drugs, we determined if key miRNAs involved in HCC etiology could be targeted by *G. sinensis* extracts. As an example, miR-21 has been shown to be critical in HCC, functioning either as a circulating biomarker¹³ or an apoptosis regulator^{14,15}. In our rat model of HCC, we determined miR-21 amounts by qRT-PCR and found that

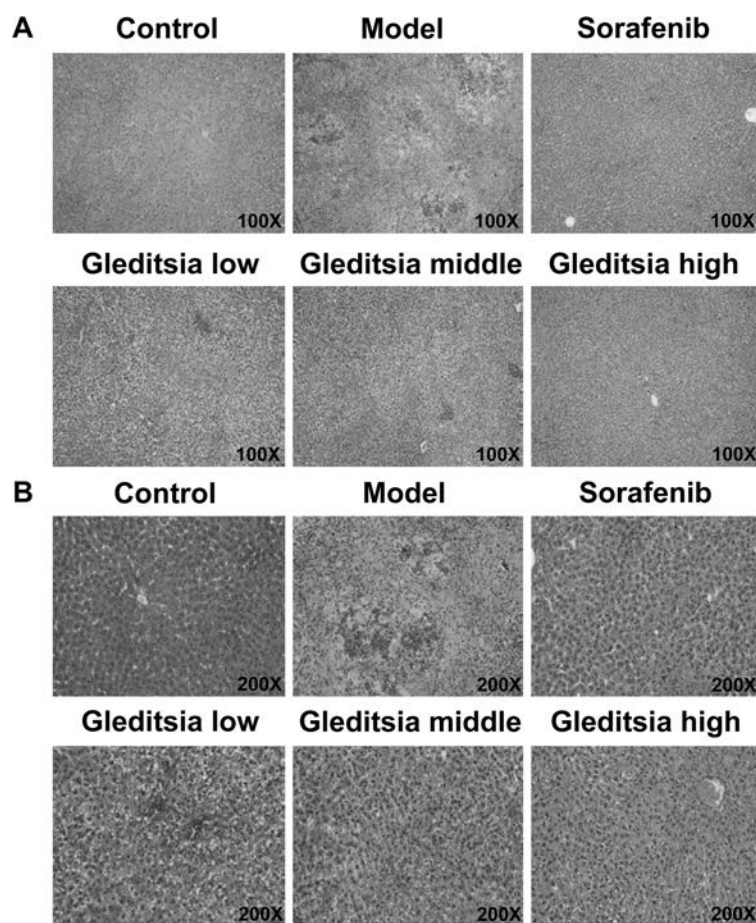


Figure 1. Histopathology of liver samples from control ($N=12$) and hepatocellular carcinoma (HCC) model rats ($N=13$), as well as HCC rats treated with *G. sinensis* extracts or sorafenib. Liver sections were examined following hematoxylin and eosin (H&E) staining. Representative sections are displayed in (A) (100×) and (B) (200×).

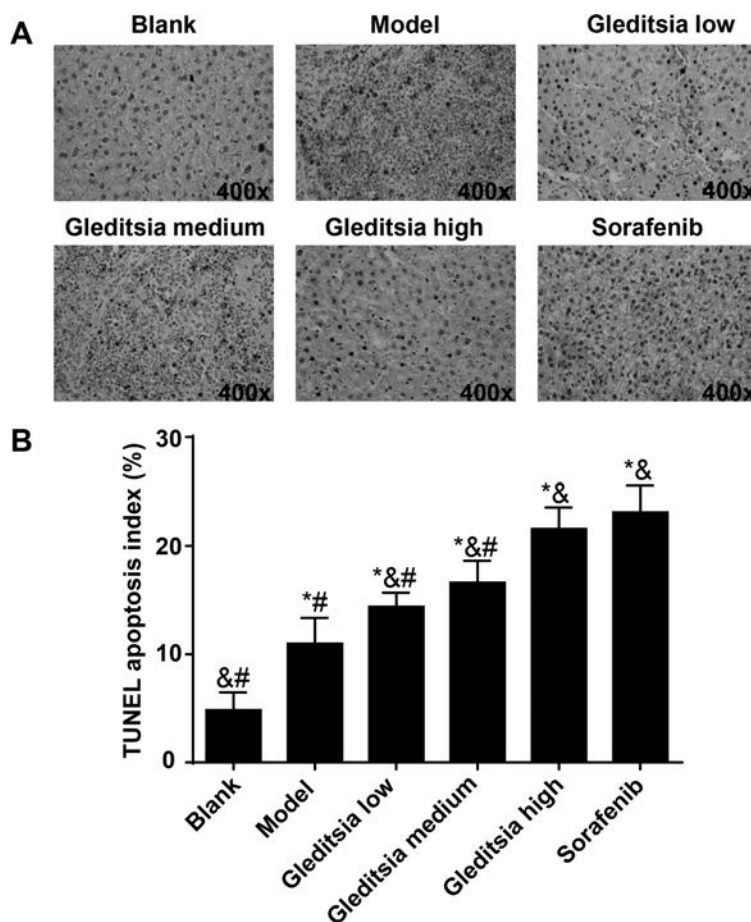


Figure 2. Apoptosis of liver cells from control ($N=12$) and HCC model rats ($N=13$), as well as HCC rats treated with *G. sinensis* extracts ($N=10$ in each dose) or sorafenib ($N=10$). (A) Apoptotic cells in liver sections were examined by TUNEL staining, displayed as dark signals. Representative sections are shown. (B) Quantification of (A); the TUNEL index is the percentage of positive cells among all cells. * $p < 0.01$ versus the control group; &# $p < 0.01$ versus the model group; # $p < 0.01$ versus the sorafenib group.

it was significantly elevated in liver tissues from HCC-bearing rats, and both *G. sinensis* extracts and sorafenib could restore the abundance of miR-21 in HCC liver tissues. This effect was dose dependent, as a higher dose of the *G. sinensis* extract caused better recovery of miR-21 (Fig. 3A).

Previous reports indicated that the conserved miR-181 family members are upregulated in a group of EpCAM⁺ HCC cells with cancer stem cell features and high invasiveness¹⁶; in addition, TGF- β -mediated upregulation of hepatic miR-181b promotes HCC progression¹⁷. Hence, we also determined the abundance of miR-181b in HCC rat liver samples with or without *G. sinensis* extract treatment. Similar to miR-21, miR-181b was significantly elevated in liver samples from HCC-bearing rats, and both *G. sinensis* extracts and sorafenib could restore the abundance of miR-181b in HCC liver tissues. This effect was also dose dependent, as a higher dose of *G. sinensis* extract caused a better recovery of miR-181b (Fig. 3B).

HCC is known to express important amounts of miR-183¹⁸. The Wnt/ β -catenin pathway could activate miR-183 expression in HCC to promote cell invasion¹⁹, and miR-183 also inhibits TGF- β 1-induced apoptosis in HCC tumor cells¹⁶. Therefore, we also determined the abundance of miR-183 in HCC rat liver tissues, with or without *G. sinensis* extract treatment. Similar to miR-21, miR-183 was significantly elevated in liver tissues from HCC-bearing rats, and both *G. sinensis* extracts and sorafenib could restore the abundance of miR-183 in HCC livers. This effect was dose dependent, as a higher dose of *G. sinensis* extract caused a better recovery of miR-183 (Fig. 3C).

Influence of Gleditsia sinensis Extracts on mRNA and Protein Levels of PTEN, TIMP3, MMP2, MMP9, and PDCD4 in HCC-Bearing Rats Toward Anticancer Activity

As miRNAs execute their biological functions by suppressing target protein expression, we were interested

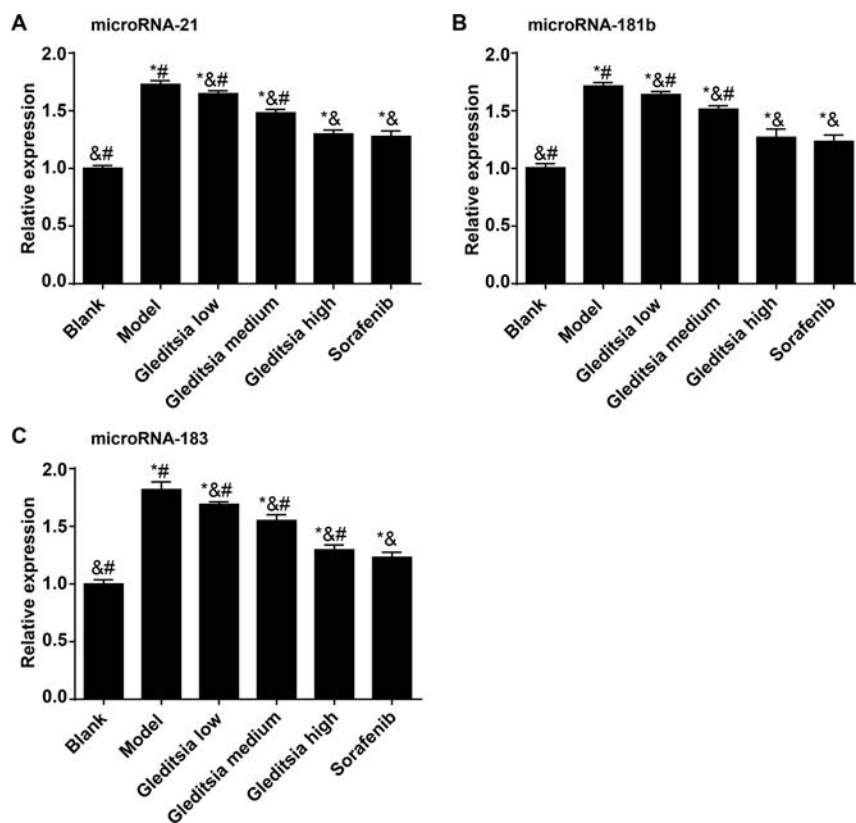


Figure 3. Abundance levels of miR-21/181b/183 in the liver from the control ($N=12$) and HCC model rats ($N=13$), as well as HCC rats treated with *G. sinensis* extracts ($N=10$ in each dose) or sorafenib ($N=10$). The abundance levels of miRNAs were determined by quantitative real-time (qRT)-PCR with specific primers. The relative abundance levels of miR-21 (A), miR-181b (B), and miR-183 (C) are shown. * $p < 0.01$ versus the control group; & $p < 0.01$ versus the model group; # $p < 0.01$ versus the sorafenib group.

in determining the target proteins affected by miR-21/181b/183 involved in treatment effects of *G. sinensis* extracts in HCC-bearing rats. The inhibition of PTEN expression by miR-21 has been widely reported, and multiple downstream functions of PTEN, like migration²⁰, autophagy²¹, and apoptosis²², could be affected by miR-21 in HCC cells. Hence, we determined PTEN expression in HCC rat liver tissues after treatment with *G. sinensis* extracts. We found that PTEN was significantly reduced in liver samples from HCC-bearing rats, and both *G. sinensis* extracts and sorafenib could restore the levels of PTEN in HCC liver tissues. This effect was dose dependent, as a higher dose of *G. sinensis* extract caused a better recovery of PTEN. These effects were observed both at the mRNA and protein levels (Fig. 4A, F, and G).

Similarly, we assessed the expression of TIMP3, a validated target of miR-181b in HCC¹⁷, in model rat livers. We found that TIMP3 was significantly reduced in liver samples from HCC-bearing rats, and both *G. sinensis* extracts and sorafenib could restore the levels of TIMP3 in HCC liver tissues. This effect was also dose dependent, as a higher dose of *G. sinensis* extract caused

a better recovery of TIMP3. These effects were observed both at the mRNA and protein levels (Fig. 4B, F, and H). As TIMP3 is a potent inhibitor of matrix metalloproteinases (MMPs) in HCC¹⁷, we investigated whether *G. sinensis* extracts also affected MMP expression. The expression levels of both MMP-2 (Fig. 4C, F, and I) and MMP-9 (Fig. 4D, F, and J) were significantly increased in liver samples from HCC-bearing rats, and both *G. sinensis* extracts and sorafenib could restore the amounts of PTEN in HCC liver tissues. These effects were dose dependent, as a higher dose of *G. sinensis* extract caused a better recovery. These effects were again observed both at the mRNA and protein levels.

Finally, we determined the expression of PDCD4, a reported miR-183 target in HCC¹⁶, in model rat livers. We found that PDCD4 was significantly reduced in liver samples from HCC-bearing rats, and both *G. sinensis* extracts and sorafenib could restore the levels of PDCD4 in HCC liver tissues. These effects were dose dependent, as a higher dose of *G. sinensis* extract caused a better recovery of PDCD4. These effects were observed at both the mRNA and protein levels (Fig. 4E, F, and K).

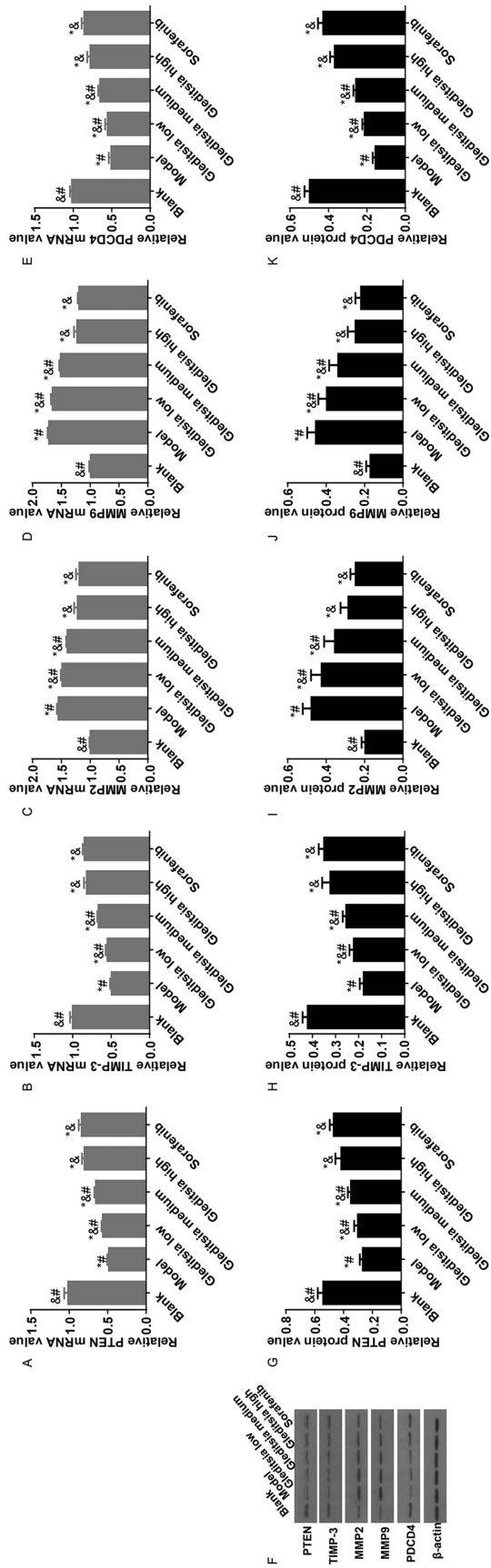


Figure 4. Abundance levels of PTEN, TIMP3, MMP-2/9, and PDCD4 in the liver from control ($N=12$) and HCC model rats ($N=13$), as well as HCC rats treated with *G. sinensis* extracts ($N=10$ in each dose) or sorafenib ($N=10$). mRNA levels of PTEN (A), TIMP3 (B), MMP-2 (C), MMP-9 (D) and PDCD4 (E), and protein (F) levels of PTEN (G), TIMP3 (H), MMP-2 (I), MMP-9 (J), and PDCD4 (K), as determined by qRT-PCR and Western blotting, respectively. The relative abundance levels of mRNAs are displayed. * $p<0.01$ versus the control group; & $p<0.01$ versus the model group; # $p<0.01$ versus the sorafenib group.

DISCUSSION

HCC is currently the third leading cause of cancer deaths worldwide, affecting more than 500,000 people. The incidence of HCC is highest in Asia and Africa, where the endemic high prevalence of hepatitis B and hepatitis C leads to a high risk of chronic liver disease and subsequent development of HCC^{23,24}. Hence, developing an effective therapeutic strategy for patients with end-stage liver disease and HCC is a significant focus, given the fact that many patients are not suitable for liver transplantation. During the past years, there has been an extensive effort to harness traditional Chinese medicine in clinical HCC management, and a meta-analysis indicated the therapeutic potential of such a great natural resource in HCC²⁵. Therefore, we need to dissect detailed components of Chinese herbal drugs for effective HCC treatment, and analyze the underlying molecular and cellular mechanisms, in order to further promote their application in HCC clinical therapeutics.

G. sinensis extracts have been reported as effective anticancer drugs for HCC during the past years. The extracts significantly inhibit cell proliferation in the human HCC bel-7402 cell line, by inducing apoptosis, inhibiting telomerase activity, regulating activation of tumor suppressor genes, and inactivating oncogenes²⁶. *G. sinensis* extract also upregulates Smad4 mRNA expression and downregulates Smad7 mRNA expression in liver tissues of tumor-bearing mice, thus enhancing transactivation of the TGF- β /Smads signal transduction pathway and playing an inhibitory role in HCC cell proliferation^{27,28}. In addition, *G. sinensis* extract could reduce vascular endothelial growth factor (VEGF) mRNA expression in HepG2 hepatoblastoma cell lines, thereby demonstrating a potential to reduce the angiogenic activity of basic fibroblast growth factor in HCC²⁹.

In the present study, we established an HCC model in rats via implantation of cancerous Walker-256 cells and examined the therapeutic effects of *G. sinensis* extracts. The histopathology of liver sections, as well as TUNEL apoptosis detection, indicated that *G. sinensis* extracts significantly suppressed HCC progression in the rat liver, possibly by inducing apoptosis in cancer cells. We treated the HCC rats with sorafenib, a commonly used drug for treating HCC, as a positive control, and found that a high dose of *G. sinensis* extract could be as efficient as sorafenib, while its toxicity was indeed minimal³⁰. Our findings corroborate previous studies demonstrating the anticancer activity of *G. sinensis* in animal models^{6,7}. In agreement, it was previously shown that multiple compounds purified from the thorns of *G. sinensis* induce apoptosis in human breast (MCF 7)³¹ and liver (SK-hep-1)³² cancer cells.

Given the limited *G. sinensis* studies in HCC, especially in in vivo models, it remains unclear whether *G. sinensis* could be an efficient treatment for HCC. It is known that miRNAs play essential roles in the pathogenesis of almost every type of cancer, as revealed by numerous reports on differentially regulated miRNAs in various cancers, as well as the importance of exosomes, which was stressed upon. As carriers for intercellular information exchange, including miRNA trafficking, the potential role of extracellular vesicles (or exosomes) in HCC formation, progression, and therapy has been widely explored³³. The miRNA profile in serum exosomes in HCC patients is significantly altered compared with that of patients with chronic hepatitis B and liver cirrhosis, including both upregulated and downregulated miRNA species^{34,35}. Wei et al.³⁵ further demonstrated that Vps4A, a key regulator of exosome biogenesis, is downregulated in HCC tissues, while Vps4A suppresses HCC cell tumorigenesis by facilitating the secretion of oncogenic miRNAs in exosomes as well as the accumulation and uptake of tumor suppressor miRNAs in cells. The miRNAs affected by Vps4A collectively regulate the phosphatidylinositol-3-kinase/Akt signaling pathway. Moreover, stromal cells in HCC also secrete exosomal miRNAs to control tumor cells. Exosomes derived from HCC cancer-associated fibroblasts contain significantly reduced miR-320a, which could target the MAPK pathway to restrain tumor cell growth³⁶.

Considering the importance of miRNAs in mediating HCC pathogenesis, we determined several key miRNAs in HCC rat models. These miRNAs were previously reported to be critical in HCC animal models or patients, and their protein targets were demonstrated to be essential for HCC progression. The miR-21/PTEN axis controls multiple biological pathways, including migration²⁰, autophagy²¹ and apoptosis²², all of which contribute to tumorigenesis. Hence, *G. sinensis* might exert anticancer effects by modulating miR-21/PTEN signaling. In addition to PTEN, PDCD4 is another player in HCC cell apoptosis. In the present study, we found that miR-183, the regulatory miRNA of PDCD4, was elevated in the HCC rat liver, and this elevation was restored by treatment with *G. sinensis* extract. The parallel alteration of PDCD4 was detected in the current HCC rats, indicating the participation of miR-183/PDCD4 signaling in HCC. Similarly, the miR-181b/TIMP3 axis was previously reported in an HCC model, concluding that the inhibitory effect of TIMP3 on MMPs might prevent tumor progression¹⁷. Here we showed that *G. sinensis* extract significantly altered the expression of miR-181b, TIMP3, and MMP-2/9, indicating an active involvement of this molecular pathway in the therapeutic effect of *G. sinensis* extract in HCC. Interestingly, the regulatory effects of *G. sinensis* extract on MMP-2 and MMP-9 have been previously reported⁸.

Overall, this study confirmed the therapeutic effects of *G. sinensis* extract on HCC in a rat Walker-256 cell transplantation model, and *G. sinensis* extract could be as efficient as sorafenib, which is currently used for HCC worldwide. We found that *G. sinensis* extract dramatically induced apoptosis in the HCC liver. These effects might be attributed to miRNAs. Indeed, miR-21/181b/183 was upregulated in the HCC liver in this study, and their levels were restored by both *G. sinensis* extract and sorafenib. Consistently, we found downregulation of PTEN/TIMP3/PDCD4, the targets of miR-21/181b/183, in the HCC liver, and the alteration of these genes could be restored by both *G. sinensis* extract and sorafenib. The effects of TIMP3 on MMP-2/9 expression were also determined. The present findings further indicate the potential of *G. sinensis* extract in HCC treatment, expanding the understanding of molecular mechanisms by which miRNAs participate in the anti-HCC effect of *G. sinensis* extract.

ACKNOWLEDGMENTS: This study was supported by grants from the Chinese Academy of Traditional Chinese Medicine (No. 2011XYCZ-13) and the Hubei Province Natural Science Foundation Project (No. 2012FFC042). The authors declare no conflicts of interest.

REFERENCES

- Zhang JP, Tian XH, Yang YX, Liu QX, Wang Q, Chen LP, Li HL, Zhang WD. Gleditsia species: An ethnomedical, phytochemical and pharmacological review. *J Ethnopharmacol.* 2016;178:155–71.
- Gao J, Yang X, Yin W. From traditional usage to pharmacological evidence: A systematic mini-review of Spina Gleditsiae. *Evid Based Complement Alternat Med.* 2016; 2016:3898957.
- Li J, Jiang K, Wang LJ, Yin G, Wang J, Wang Y, Jin YB, Li Q, Wang TJ. HPLC-MS/MS determination of flavonoids in Gleditsiae Spina for its quality assessment. *J Sep Sci.* 2018;41(8):1752–63.
- Yu J, Xian Y, Li G, Wang D, Zhou H, Wang X. One new flavanocoumarin from the thorns of Gleditsia sinensis. *Nat Prod Res.* 2017;31(3):275–80.
- Kim KH, Han CW, Yoon SH, Kim YS, Kim JI, Joo M, Choi JY. The fruit hull of Gleditsia sinensis enhances the anti-tumor effect of cis-diammine dichloridoplatinum II (Cisplatin). *Evid Based Complement Alternat Med.* 2016; 2016:7480971.
- Ryu S, Park KM, Lee SH. Gleditsia sinensis thorn attenuates the collagen-based migration of PC3 prostate cancer cells through the suppression of alpha2beta1 integrin expression. *Int J Mol Sci.* 2016;17(3):328.
- Yi JM, Kim J, Park JS, Lee J, Lee YJ, Hong JT, Bang OS, Kim NS. In vivo anti-tumor effects of the ethanol extract of Gleditsia sinensis thorns and its active constituent, cytochalasin H. *Biol Pharm Bull.* 2015;38(6):909–12.
- Melek FR, Aly FA, Kassem IA, Abo-Zeid MA, Farghaly AA, Hassan ZM. Three further triterpenoid saponins from Gleditsia caspica fruits and protective effect of the total saponin fraction on cyclophosphamide-induced genotoxicity in mice. *Z Naturforsch C.* 2015;70(1–2):31–7.
- Ghouri YA, Mian I, Rowe JH. Review of hepatocellular carcinoma: Epidemiology, etiology, and carcinogenesis. *J Carcinog.* 2017;16:1.
- Shimizu D, Inokawa Y, Sonohara F, Inaoka K, Nomoto S. Search for useful biomarkers in hepatocellular carcinoma, tumor factors and background liver factors (Review). *Oncol Rep.* 2017;37(5):2527–42.
- Huan L, Liang LH, He XH. Role of microRNAs in inflammation-associated liver cancer. *Cancer Biol Med.* 2016;13(4):407–25.
- Shao CW, Wang PJ, Tian JM, Zhang HJ, Wang MJ, Zeng H. Immediate injection method on making rat liver tumor model. *Chin J Med Imag Technol.* 2002;8731–2 (in Chinese).
- Guo X, Lv X, Lv X, Ma Y, Chen L, Chen Y. Circulating miR-21 serves as a serum biomarker for hepatocellular carcinoma and correlated with distant metastasis. *Oncotarget* 2017;8(27):44050–8.
- Najafi Z, Sharifi M, Javadi G. Degradation of miR-21 induces apoptosis and inhibits cell proliferation in human hepatocellular carcinoma. *Cancer Gene Ther.* 2015;22(11): 530–5.
- Yin D, Wang Y, Sai W, Zhang L, Miao Y, Cao L, Zhai X, Feng X, Yang L. HBx-induced miR-21 suppresses cell apoptosis in hepatocellular carcinoma by targeting interleukin-12. *Oncol Rep.* 2016;36(4):2305–12.
- Wang S, Cui S, Zhao W, Qian Z, Liu H, Chen Y, Lv F, Ding HG. Screening and bioinformatics analysis of circular RNA expression profiles in hepatitis B-related hepatocellular carcinoma. *Cancer Biomark.* 2018;22(4):631–40.
- Wang B, Hsu SH, Majumder S, Kutay H, Huang W, Jacob ST, Ghoshal K. TGFbeta-mediated upregulation of hepatic miR-181b promotes hepatocarcinogenesis by targeting TIMP3. *Oncogene* 2010;29(12):1787–97.
- Xu C, Luo L, Yu Y, Zhang Z, Zhang Y, Li H, Cheng Y, Qin H, Zhang X, Ma H, Li Y. Screening therapeutic targets of ribavirin in hepatocellular carcinoma. *Oncol Lett.* 2018;15(6):9625–32.
- Leung WK, He M, Chan AW, Law PT, Wong N. Wnt/beta-catenin activates MiR-183/96/182 expression in hepatocellular carcinoma that promotes cell invasion. *Cancer Lett.* 2015;362(1):97–105.
- Hu L, Ye H, Huang G, Luo F, Liu Y, Liu Y, Yang X, Shen J, Liu Q, Zhang J. Long noncoding RNA GAS5 suppresses the migration and invasion of hepatocellular carcinoma cells via miR-21. *Tumour Biol.* 2016;37(2):2691–702.
- He C, Dong X, Zhai B, Jiang X, Dong D, Li B, Jiang H, Xu S, Sun X. MiR-21 mediates sorafenib resistance of hepatocellular carcinoma cells by inhibiting autophagy via the PTEN/Akt pathway. *Oncotarget* 2015;6(30):28867–81.
- Zhang K, Chen J, Chen D, Huang J, Feng B, Han S, Chen Y, Song H, De W, Zhu Z, Wang R, Chen L. Aurora-A promotes chemoresistance in hepatocellular carcinoma by targeting NF-kappaB/microRNA-21/PTEN signaling pathway. *Oncotarget* 2014;5(24):12916–35.
- Bertuccio P, Turati F, Carioli G, Rodriguez T, La Vecchia C, Malvezzi M, Negri E. Global trends and predictions in hepatocellular carcinoma mortality. *J Hepatol.* 2017;67(2): 302–9.
- Johnson P, Berhane S, Kagebayashi C, Satomura S, Teng M, Fox R, Yeo W, Mo F, Lai P, Chan SL, Tada T, Toyoda H, Kumada T. Impact of disease stage and aetiology on survival in hepatocellular carcinoma: Implications for surveillance. *Br J Cancer* 2017;116(4):441–7.

25. Yang Z, Liao X, Lu Y, Xu Q, Tang B, Chen X, Yu Y. Add-on therapy with traditional Chinese medicine improves outcomes and reduces adverse events in hepatocellular carcinoma: A meta-analysis of randomized controlled trials. *Evid Based Complement Alternat Med*. 2017;2017:3428253.
26. Zhang ZY, Zhang CZ, Xu HL, Zhu QJ. Influence of *Gleditsia sinensis* Lam extractive on the regulation of cancerous gene and telomerase activity of human hepatocarcinoma cell. *Chin J Integr Trad Western Med Liver Dis*. 2008;18(2):93–5 (in Chinese).
27. Du JJ, Zhang CZ, Xu HL, Wang HW, Fei XY, Li SL. *Gleditsia* extract in mice hepatoma cells TGF- β /Smads regulation of signaling system. *Chin J Integr Trad Western Med Liver Dis*. 2010;20(3):164–5 (in Chinese).
28. Peng WJ, Lu DB. Regulatory role of *Gleditsia sinensis* extract to TGFbeta-1 mRNA expression in liver tumor cells. *Hubei J Trad Chin Med*. 2010;32(5):6–8 (in Chinese).
29. Chow LM, Chui CH, Tang JC, Lau FY, Yau MY, Cheng GY, Wong RS, Lai PB, Leung TW, Teo IT, Cheung F, Guo D, Chan AS. Anti-angiogenic potential of *Gleditsia sinensis* fruit extract. *Int J Mol Med*. 2003;12(2):269–73.
30. Lu DB, Zhang CZ. Chronic toxicity of *Gleditsia sinensis* extract in rats. *J Hubei Coll Trad Chin Med*. 2013;15(6):16–9 (in Chinese).
31. Yu J, Li G, Mu Y, Zhou H, Wang X, Yang P. Anti-breast cancer triterpenoid saponins from the thorns of *Gleditsia sinensis*. *Nat Prod Res*. 2018:1–6.
32. Yu J, Xian Y, Li G, Wang D, Zhou H, Wang X. One new flavanocoumarin from the thorns of *Gleditsia sinensis*. *Nat Prod Res*. 2017;31(3):275–80.
33. Yang N, Li S, Li G, Zhang S, Tang X, Ni S, Jian X, Xu C, Zhu J, Lu M. The role of extracellular vesicles in mediating progression, metastasis and potential treatment of hepatocellular carcinoma. *Oncotarget* 2017;8(2):3683–95.
34. Sohn W, Kim J, Kang SH, Yang SR, Cho JY, Cho HC, Shim SG, Paik YH. Serum exosomal microRNAs as novel biomarkers for hepatocellular carcinoma. *Exp Mol Med*. 2015;47:e184.
35. Wei JX, Lv LH, Wan YL, Cao Y, Li GL, Lin HM, Zhou R, Shang CZ, Cao J, He H, Han QF, Liu PQ, Zhou G, Min J. Vps4A functions as a tumor suppressor by regulating the secretion and uptake of exosomal microRNAs in human hepatoma cells. *Hepatology* 2015;61(4):1284–94.
36. Zhang Z, Li X, Sun W, Yue S, Yang J, Li J, Ma B, Wang J, Yang X, Pu M, Ruan B, Zhao G, Huang Q, Wang L, Tao K, Dou K. Loss of exosomal miR-320a from cancer-associated fibroblasts contributes to HCC proliferation and metastasis. *Cancer Lett*. 2017;39733–42.